

## Blastwave parameters assessment at different altitude using numerical simulation

Ramezan Ali IZADIFARD<sup>1</sup>, Mohsen FOROUTAN<sup>2</sup>

<sup>1</sup>*IK University-IRAN*

*e-mail: Izadifard @ ikiu.ac.ir*

<sup>2</sup>*Koosha Paydar Consulting Engineers CO, IRAN*

Received 22.11.2009

### Abstract

There are some equations to establish the relationship between blastwave parameters with scaled distance. In this paper, the resulting data from numerical simulations by AUTODYN-1D for different marked distances from detonation points and different amounts of charge are compared with results from experimental data and equations. To sum up, some equations for evaluating blastwave parameters are presented, which are in excellent conformity with numerical and experimental data. In addition, the importance of the effect of altitude from sea level is clearly expressed and the presented equations are modified by proposing a modifying coefficient.

**Key Words:** Overpressure, Duration, Impulse, Blastwave Parameters, Altitude

### Introduction

A great amount of energy is released in a matter of seconds with the explosion of high density explosive material. The pressure of the hot gases produced by this reaction is some 100-300 Kbar and its temperature is about 3000-4000 °C (Smith and Hetherington, 1994). Expansion of these produced gases with initial velocity, which varies from 1800 to 9100 m/s, causes movement of ambient atmosphere. Because of this, a layer of compressed air will form in front of these gases. This layer is called the blastwave and is known by its parameters such as maximum overpressure, impulse, and duration (Mays and Smith, 1995; Krauthammer, 2008).

Force applied by the blastwave and the loading rate can be calculated when the parameters of the blastwave are known. These parameters are very important in designing structures to withstand explosive loading. Therefore, an equation of movement for the shockwave is mandatory, but it requires very complicated calculations. The most important aspects of an explosion are the calculation of overpressure, duration, and impulse at a certain standoff distance from the detonation point.

As the blastwave gradually moves away from the detonation point, its pressure drops significantly and becomes equal to the atmospheric pressure. The blastwave generated loses its initial heat and velocity by the time it reaches a distance approximately 40 to 50 times the diameter of the charge from the detonation point (Mays and Smith, 1995). Changes in the pressure of a point at a certain distance from the explosive with

respect to time are shown in Figure 1. The generated blastwave contains 2 phases; a positive one, which is called pressure, and a negative one, which is called suction (Smith and Hetherington, 1994). The absolute difference between the produced pressure and the pressure of the environment is called overpressure and is greater and more important than the suction phase. Therefore, only the positive phase is considered in the loading of structures (Smith and Hetherington, 1994; Mays and Smith, 1995; Bangash and Bangash, 2006; Krauthammer, 2008). The area between overpressure and time axes is impulse and the time interval in which pressure is more than the ambient pressure is called duration.

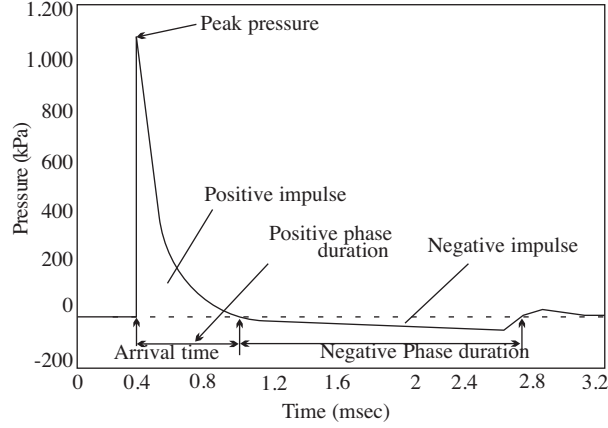


**Figure 1.** Blastwave pressure-time profile.

It can be seen in Figure 1 that the overpressure will decay after it reaches its maximum. The rate of the decay of the overpressure with respect to time can be approximated with an exponential function called a Friendlander curve (Eq. (1)) (Bulson, 1997):

$$P = P_s \left[ 1 - \frac{t}{T_s} \right] e^{-\alpha t/T_s} \quad (1)$$

where  $P$  is the overpressure in time  $t$ ,  $P_s$  is the maximum overpressure,  $T_s$  is the positive phase duration, and  $\alpha$  is a coefficient that shows the decay of the curve.

Brode, for the first time, established analytically an equation for shockwave calculation and presented a semi-analytical equation for maximum overpressure (Smith and Hetherington, 1994). Accordingly, equation adjunctions and modifications were performed by other researchers (Smith and Hetherington, 1994). The equation of the explosion phenomenon has been developed by Henrych (1979) with investigating the frontal shockwave within the charge, air, and interface and on the basis of satisfying the boundary and initial conditions. Moreover, he presented an equation for calculating the maximum overpressure. Kinney and Graham (1985) presented equations for estimating the maximum overpressure, duration, and impulse. Furthermore, Izadifard and Maheri (2010) suggested an equation for calculating  $T_s$ .

All equations use scaled distance ( $Z$ ) for calculating the parameters, which is derived by Eq. (2):

$$Z = \frac{R}{W^{1/3}} \quad (2)$$

where  $R$  represents the distance from the detonation point in meters and  $W$  is the mass of TNT charge in

kilograms (for other kinds of charges than TNT, coefficient of equivalent mass of TNT can be used, refer to TM5-855-1 (1987)).

In order to calculate blastwave parameters versus scaled distance, in structural design applications, some graphs are presented to be employed; refer to TM5-1300 (1990) and UFC-3-340-02 (2008). These graphs, which are presented in the report of the weapons effects calculation program CONWEP, are the results of numerous field experiments. Therefore, they can be used instead of experimental results for designing resistance to blastwave.

In this paper, blastwave parameters for different scaled distances and altitudes are calculated by numerical simulations.

### **Blastwave Numerical Simulation**

As mentioned before, many semi-experimental equations have been submitted in order to measure blastwave parameters at different standoff points. These equations are presently used for overpressure assessment in research and design. With advancement and extraordinary versatility of software packages to perform numerical simulations, many researchers have tried to employ the hydrocode in order to estimate explosion parameters.

Clutter and Stahl (2004) used CEBAM hydrocode to model the shockwave and calculated maximum overpressure in a few specific points at different designated places. In addition, Luccioni et al. (2006) used the 3D model of AUTODYN to calculate overpressure parameters and compared maximum overpressure with Henrych's equation. Chapman et al. (1995) compared the amount of overpressure parameters derived from CONWEP with the results of 2D simulation in AUTODYN. Moreover, it is concluded from the above-mentioned references that the presumption of the above-mentioned software is suitable for modeling such a phenomenon. In addition, Borgers and Vantomme (2006) used AUTODYN for modeling planar blastwave created with a detonating cord.

Considering that an explosion of spherical charge has physical and geometrical symmetry in the  $\theta$  and  $\phi$  directions  $\theta\phi$ , it is possible to be examined in hydrocode software by one-dimensional analysis. In this paper, AUTODYN software is used for numerical examination of any charge, because of the ability of this software in symmetrical modeling. AUTODYN hydrocode is a software package that uses finite difference, finite volume, and finite element technique for solving non-linear problems. Euler processor was used for modeling explosions. AUTODYN uses the explicit method for solving equations.

In a more complicated situation, in order to increase the accuracy, it is necessary to increase the number of elements to obtain acceptable answers. Moreover, increasing the number of elements will take a considerable amount of time. Therefore, in AUTODYN software, it is possible to have an axisymmetric simulation in relation to the importance of pressure distribution at marked intervals from detonated points. Afterwards, the pressure distribution will be inserted into the main framework (AUTODYN User's Manual, 2005).

Since the design of pressure distribution is one-dimensional, smaller elements can be used and consequently the required time to solve the problem decreases. One-dimensional simulation in AUTODYN is done in the shape of a wedge. The angle of the wedge is defined by AUTODYN and the users should only define the length of the wedge. A schematic diagram of the wedge is shown in Figure 2.

Taking into consideration the nature of the charge and surrounding air, the analysis of this problem is done using the Euler method. Therefore, wedge dimensions are always constant and it will be filled with air and charge. Moreover, the radius of the charge can be selected arbitrarily. However, attention should be paid to reflective boundary conditions at the end of the wedge and to the fact that the length of the wedge must be bigger than the projected distance, in order to obtain accurate results. It is necessary that waves should not

be reflected back from the wide end of the wedge. In fact, detonation starts from the vertex of the wedge and waves gradually move away from the vertex and distribute throughout the wedge.

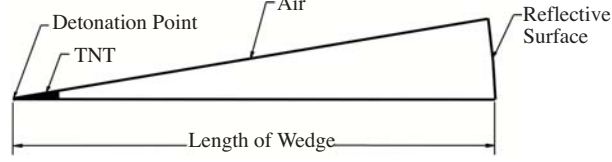


**Figure 2.** One-dimensional wedge model in AUTODYN.

The applied equation of state of ideal gas for air substance and its equation are as follows:

$$P = (\gamma - 1) \rho e + P_{shift} \quad (3)$$

In this equation,  $\gamma$  is the adiabatic exponent,  $\rho$  represents air density,  $e$  is internal air energy, and  $P_{shift}$  represents original gas pressure. The JWL equation of state is applied to calculate TNT charge. Currently, the JWL equation of state is the most suitable equation used for different charges. In addition, it can be applied to calculate the pressure reduction of up to 1 Kbar. The JWL equation of state is as follows:

$$P = C_1 \left[ 1 - \frac{w}{r_1 v} \right] e^{-r_1 v} + C_2 \left[ 1 - \frac{w}{r_2 v} \right] e^{-r_2 v} + \frac{we}{v} \quad (4)$$

In this equation,  $C_1$ ,  $C_2$ ,  $r_1$ ,  $r_2$ , and  $w$  are constant values,  $v$  is the specific volume of the charge, and  $e$  is the internal energy of the charge. In this paper, the physical properties of the air and TNT charge are shown in Tables 1 and 2, respectively, according to the AUTODYN library.

**Table 1.** Air properties (ideal gas equation of state).

Variable	Value	Unit
Reference density	1.225	kg/m <sup>3</sup>
Gamma	1.40	-
Reference Temperature	288	K
Specific Heat	0.000718	kJ/gK

**Table 2.** TNT charge properties (JWL equation of state).

Variable	Value	Unit
Reference density	1630	kg/m <sup>3</sup>
C1	374,000	MPa
C2	3750	MPa
R1	4.15	-
R2	0.09	-
w	0.35	-
C-J Detonation velocity	6.93	m/ms
C-J Energy / unit volume	6000	MJ/m <sup>3</sup>
C-J Pressure	21,000	MPa

One degree quadrilateral elements were used for modeling the wedge. To determine and investigate mesh convergence sensitivity, a 10-m long wedge and 10 kg of charge are used. The radius of charge in this case

is 0.1135 m and dimensions of elements are considered 10 mm, 5 mm, 3 mm, 2 mm, 1 mm, and 0.5 mm, respectively.

In order to determine and examine mesh convergence sensitivity, time history of pressure in  $Z$ 's equal to 0.23 m/kg<sup>1/3</sup>, 1.16 m/kg<sup>1/3</sup>, and 2 m/kg<sup>1/3</sup> for various element sizes are calculated and shown in Figure 3.

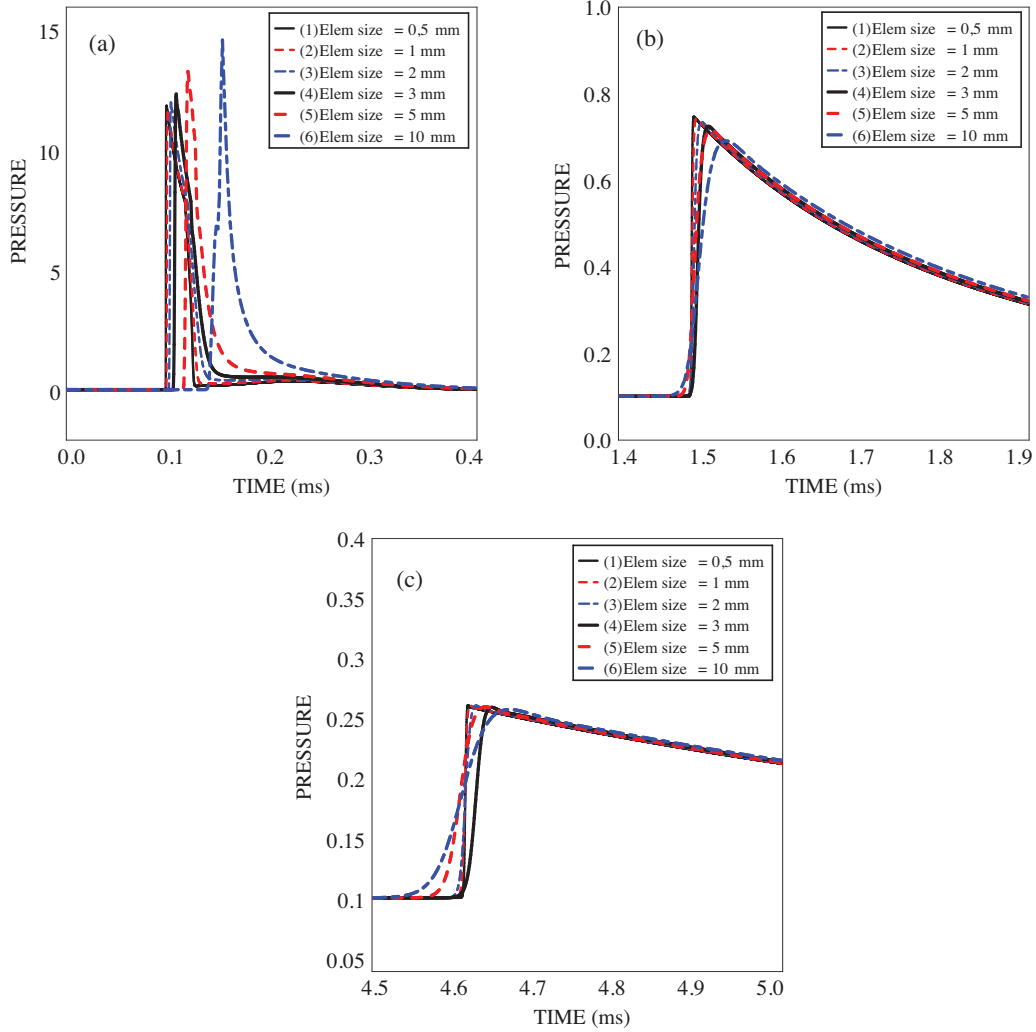


**Figure 3.** Pressure-time histories for 10 kg TNT charge at various  $Z$ s with different element size: a)  $Z = 0.23 \text{ m/kg}^{1/3}$ ; b)  $Z = 1.16 \text{ m/kg}^{1/3}$ ; c)  $Z = 2 \text{ m/kg}^{1/3}$ .

Results show that as the elements sizes become smaller the accuracy of analysis and simultaneously the solution time increase.

For small  $Z$ 's (less than 1.5), an ideal convergence will be at hand with 2 mm elements. For bigger  $Z$ 's, 3 mm or even larger dimensions will be sufficient. On the other hand, it is observed that reducing dimensions from the above-mentioned values not only causes a progressive increase in analysis time, but also the increased accuracy is insignificant. Therefore, the dimension of mesh is taken to be 1 mm in order to achieve an assured ideal accuracy for analysis and prevent any unnecessary analysis time.

**Result Extraction in Different  $Z$ 's**

A wedge with 15 m length and 15,000 elements were used to solve this problem. The length of the wedge was considered to be constant and different charge weights, e.g. 125 kg, 10 kg, 5 kg, 2 kg, and 1 kg, were used to achieve exact blastwave parameters in different  $Z$ 's. In addition, the radius of these charges were set to be 0.2635 m, 0.1135 m, 0.09013 m, 0.0641 m, and 0.05271 m, respectively.

AUTODYN software can calculate pressure at different gauges with respect to different amounts of TNT charge. Gauges are controlled points where different parameters such as pressure, velocity, and energy can be calculated. In this article these gauges are defined with a coefficient of 0.5 m intervals from each other (Figure 4).

**Maximum overpressure**

In different  $Z$ 's with different explosive weights, the relative maximum overpressures are measured and diagrams of the results are shown in Figure 5. As it can be observed from the diagram, the proximity of existing conformity is so high that all of the data can be seen as one single curve-line. The great and remarkable accuracy and proximity of correspondence, which resulted from the size of the overpressure parameter and also the slope of curvature, resulting from numerical analysis of different amount of TNT charges, collectively show that the trends of calculations by software are outstandingly correct.



**Figure 4.** Gauges' locations in AUTODYN wedge.

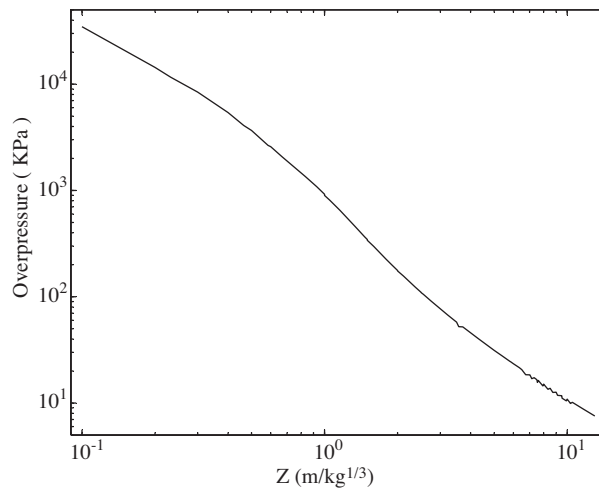


**Figure 5.** Maximum overpressure versus scaled distance (numerical results).

In Figure 6, the results from numerical analysis and the mentioned equations for calculating the maximum overpressure are compared.

All of the represented relations for calculating maximum overpressure are close to each other in higher  $Z$ 's, but in lower  $Z$ 's the difference between the results is very sensible.

In Figure 7, the results from numerical analyses with the given graph from TM5-1300 (CONWEP), which is derived from field experiment results, are compared.

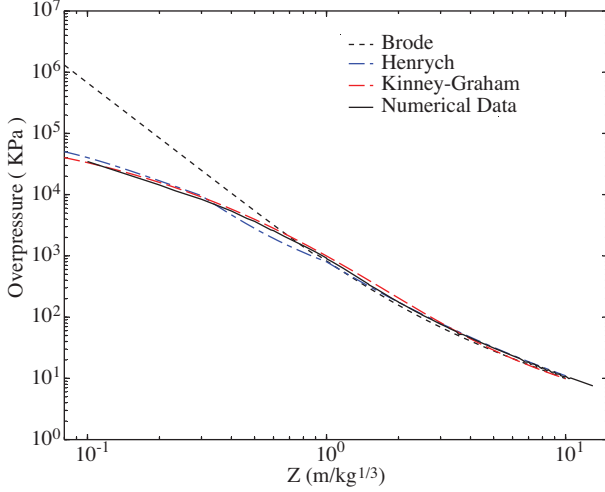


**Figure 6.** Comparison of overpressure obtained by Brode, Henrych, Kinney-Graham equations and numerical data.

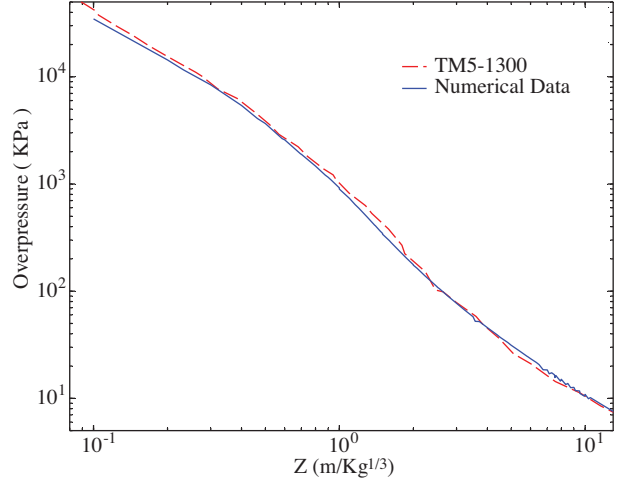


**Figure 7.** Comparison of overpressure obtained by TM5-1300 (CONWEP) and numerical data.

It can be seen from Figures 6 and 7 that the results of simulation are in good conformity with the results of the Kinney-Graham equation and TM5-1300. This conformity states that the software results are accurate and reliable.

Considering the above explanations, different diagrams have been investigated, and it was clearly indicated that the logarithmic scale distance provides us with better and more exact results. For easy calculations and great accuracy (norm of residual = 0.5), the following equation is suggested;

$$\log_{10} [\log_{10} P_s] = -0.1319X^2 - 0.3231X + 0.644 \quad (5)$$

where

$$X = \log_{10}(Z) \quad (6)$$

where  $Z$  and  $P_s$  are in terms of  $m/kg^{1/3}$  and kPa, respectively.

In Figure 8, the conformity of the results from software with Eq. (5) can be seen. This proves that the above equation can be used to calculate the maximum overpressure.

### Positive phase duration

Positive phase duration of blastwave in different  $Z$ 's is shown in Figure 9. As can be observed, the proximity of existing conformity is so high that all of the lines can be seen only as one single curve-line except in a small range. This conformity shows that these results conform to blastwave scaling law except in a small region, i.e.  $0.3 < Z < 0.4$ .

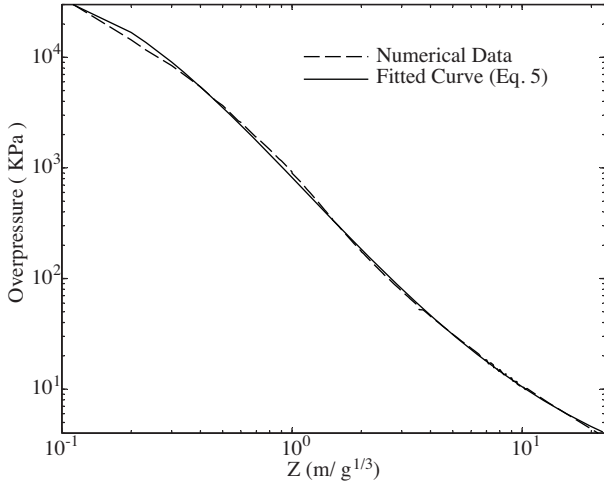


**Figure 8.** Comparison of Eq. (5) and numerical data.

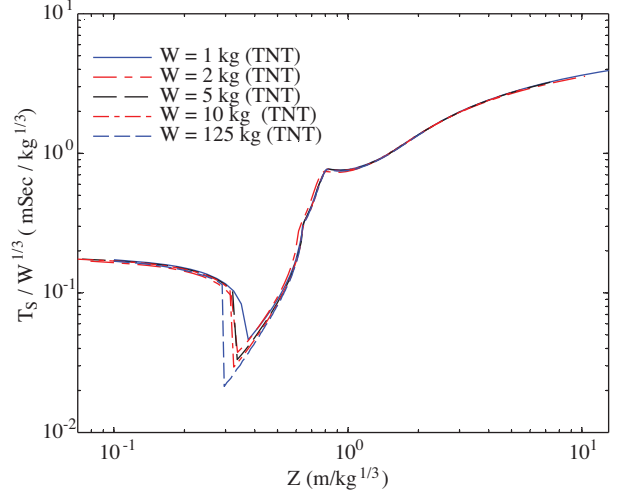


**Figure 9.** Positive phase duration for different weights versus different Z's.

Simulation results for 1 kg of TNT explosive show that the duration reaches its minimum value in Z's equal to 0.35. This decay is because of ignoring the effect of expansion of the produced gases. Increasing the weight of the explosive, the minimum value will become less and happen in smaller Z's. Examining  $T_s$  in this region, when this difference is considered, is very difficult. Therefore, one of the existing modes is considered for investigation and the results of simulation for 1 kg of TNT explosive are used. However, it should be noted that the difference in graphs for various explosives is not very great and it can be chosen arbitrarily.

$T_s$  calculated by numerical simulation and by the relation proposed by Kinney and Graham and TM5-1300 results are compared in Figure 10.

As may be seen in this figure, the difference between the Kinney-Graham equation and TM5-1300 curve is very large. These large differences can be explained by the difficulties in determining the actual end of the positive phase. The pressures decay exponentially, so that the gradient is the smallest at the zero crossing. Furthermore, measurement noise and possible disturbing signals from reflections mask the exact zero transitions. It is also seen in this figure that the value calculated by numerical simulation is higher than the results of the Kinney-Graham equation and it is less than the values of TM5-1300 results. The values of the Kinney-Graham equation in  $1 < Z < 10$  region is close to the numerical simulation results, but it deviates from simulation and TM5-1300 results in Z's greater than 10. The rate of changes in  $T_s$  is reduced in this region. It is also seen that the results of the Kinney-Graham equation in Z's smaller than 0.5 are not logical.

In order to make the calculation of positive phase duration easier, a multipart curve is fitted to the results and on this basis Eq. (7) is presented:

$$\begin{aligned}
 \frac{T_s}{W^{1/3}} &= -64.86Z^4 + 52.32Z^3 - 15.68Z^2 + 1.794Z + 0.1034 & ; & Z \leq 0.37 \\
 \frac{T_s}{W^{1/3}} &= 4.64Z^2 - 3.86Z + 0.854 & ; & 0.37 < Z < 0.82 \\
 \frac{T_s}{W^{1/3}} &= -2.97X^3 + 6.27X^2 + 0.358X + 0.763 & ; & 0.82 < Z < 2.5 \\
 \frac{T_s}{W^{1/3}} &= 0.608X^3 - 2.38X^2 + 5.62X - 0.22 & ; & Z > 2.5
 \end{aligned} \tag{7}$$



The conformity of the results of Eq. (7) and the simulation results are shown in Figure 11. According to the reliability of the results of the simulation, one can use Eq. (7) in design and investigations.

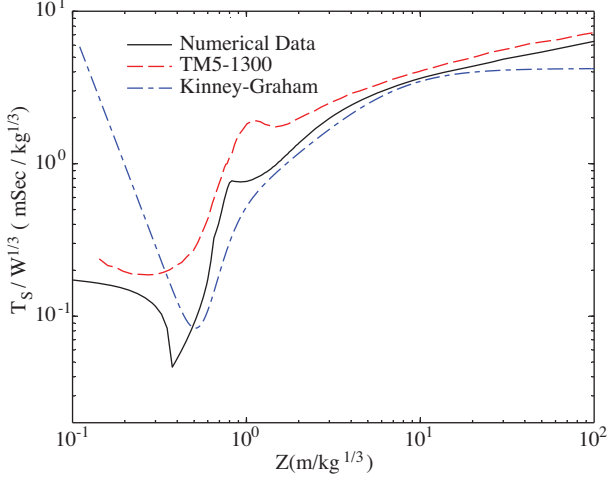


**Figure 10.** Comparison of positive phase duration obtained by simulation, Kinney-Graham equation, and TM5-1300 results.

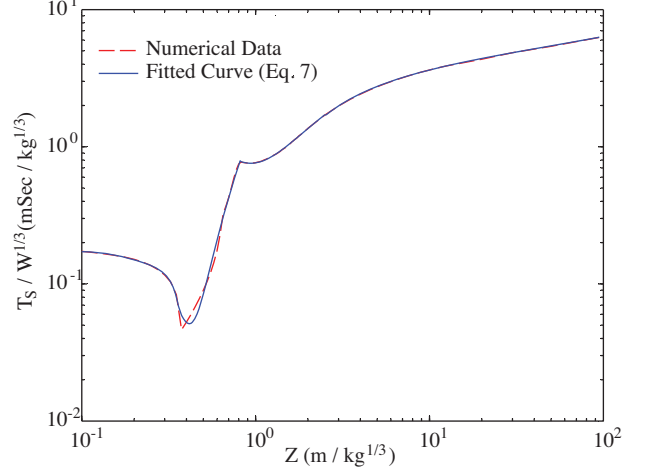


**Figure 11.** Comparison of the results of Eq. (7) and simulation.

### Positive impulse

Impulse values calculated by the numerical analysis of different masses of TNT are presented in Figure 12. It is seen in this figure that all of the graphs in the  $Z > 0.5$  range conform with each other and in  $Z < 0.5$  the differences are negligible.

Therefore, in the following investigations, numerical results of the explosion of 1 kg of TNT are respected.

In Figure 13, the impulse calculated by numerical simulation is compared with the results of the Kinney-Graham equation and TM5-1300. It is seen in this figure that the developed curve by Kinney and Graham differs a lot from TM5-1300. It is also seen that the variation process of impulse with  $Z$ 's in the equation developed by Kinney and Graham has great differences with simulation results and the TM5-1300 graph.

It is seen in Figure 13 that the results of the TM5-1300 graph are greater than the results of numerical simulation in all of the investigated range. In some references (e.g. Black, 2006; Luccioni et al., 2006;), it is emphasized that the proposed graph by TM5-1300 estimates the impulse 15% more than the value registered by field experiments. Hence,  $Z$  and impulse values of the above graph are modified and are compared with numerical results in Figure 14. Good conformity in Figure 14 shows the accuracy of numerical modeling.

Fitting an appropriate curve on the numerical results, Eq. (8) is proposed in order to calculate impulse rapidly and exactly.

$$\begin{aligned} \log_{10} (I_m / W^{1/3}) &= [-3.423 X^4 - 10.143 X^3 - 7.558 X^2 - 1.614 X + 2.14] \quad ; \quad Z < 0.8 \\ \log_{10} (I_m / W^{1/3}) &= [-0.070 X^2 - 0.853 X + 2.153] \quad ; \quad Z \geq 0.8 \end{aligned} \quad (8)$$

in which the dimension of  $I_m$  is Pa-s.

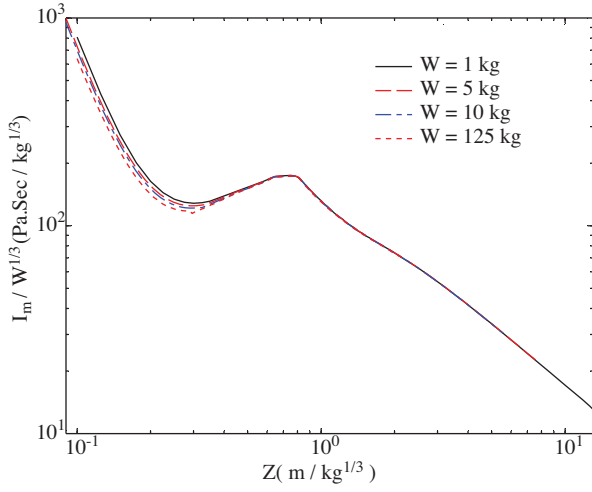


**Figure 12.** Positive impulse for different weights versus different Z's.

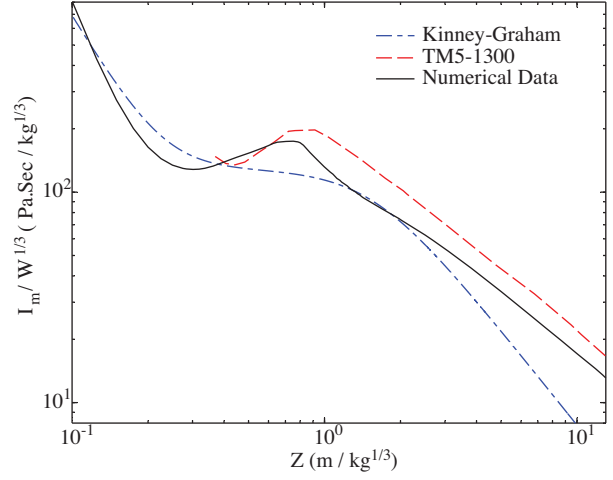


**Figure 13.** Comparison of impulse obtained by simulation, Kinney-Graham equation, and TM5-1300 results.

In Figure 15, numerical simulation results are compared with the graph of proposed Eq. (8). This comparison shows that Eq. (8) can certainly be used for positive impulse calculations.

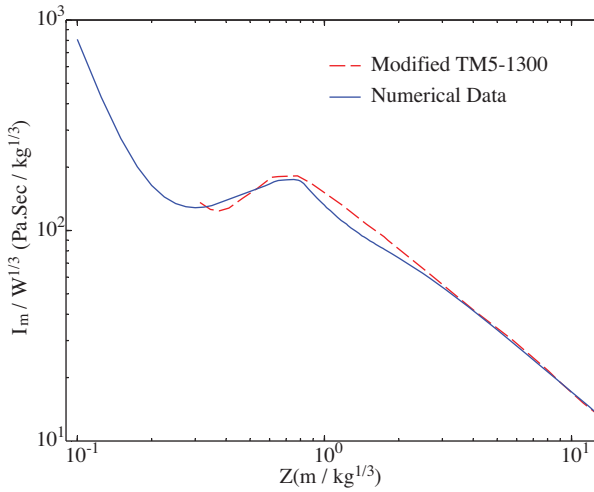


**Figure 14.** Comparison of impulse obtained by simulation and modified TM5-1300 results.

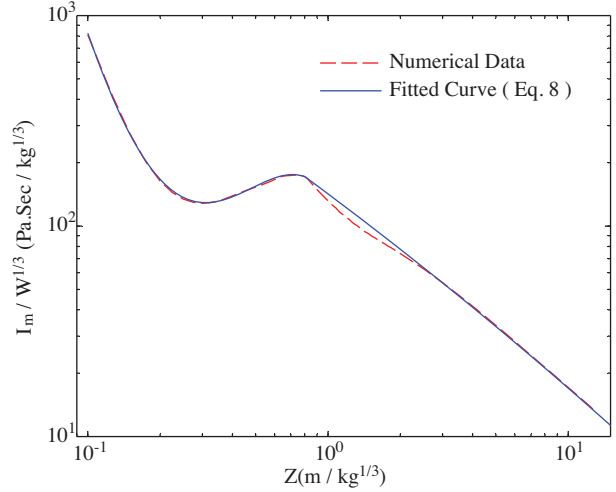


**Figure 15.** Comparison of the results of Eq. (8) and simulation.

### An Examination of Altitude Effects on Blastwave Parameters

In many of the discussed and submitted equations, the gathered data are only applicable when we have standard conditions at sea level, presented in Table 3. An interesting point that we should pay attention to is the fact that as the ambient pressure increases the produced gases from the explosion become more confined and, consequently, the pressure of such gases increases, and its blastwaves carry much more pressure. Since many places in the world are situated at elevations higher than sea level, the ambient pressure and overpressure in these areas is less compared to that at sea level.

**Table 3.** Values of parameters at sea level.

Temperature (°C)	Air density (kg/m <sup>3</sup> )	Ambient pressure (Pa)	Height above sea level (m)
15	1.225	101,332	0

Henrych, Kinney, and Graham investigated the effect of ambient pressure in their equations on maximum overpressure. They developed their equations based on normalized pressure. The results of the mentioned equations for zero elevation were examined in the previous section. The results for different altitudes are not compared in any other references. In Figure 16, the resulting pressure from Henrych and Kinney-Graham equations for 3 different elevations (0, 2000, and 5000 m) are shown. It is obvious that the maximum overpressure difference, estimated by the above equations, due to altitude difference is very great.

The ambient pressure at different altitudes can be derived from the following equation (Shames, 1982):

$$P_0 = 101332 \exp \left( -\frac{11.99}{101332} h \right) \quad (9)$$

In this equation,  $h$  is elevation in meters and  $P_0$  is in Pa.

It is necessary that other parameters and factors be equal in order to calculate the effect of altitude on overpressure. Therefore, temperatures of the locality at all times and conditions are considered to be 15 °C. The calculation of the produced internal energy of particles is as follows:

$$e = C_v T \quad (10)$$

where  $C_v$  is specific heat at constant volume and in the ideal gas, such as air, depends only on temperature (Sonntag, 1998). Since the temperature is constant, it can be concluded that the internal energy is also constant at all times and conditions. Therefore, the following equation can be used to calculate density at different altitudes:

$$\rho_h = \frac{p_h}{p_0} \rho_0 \quad (11)$$

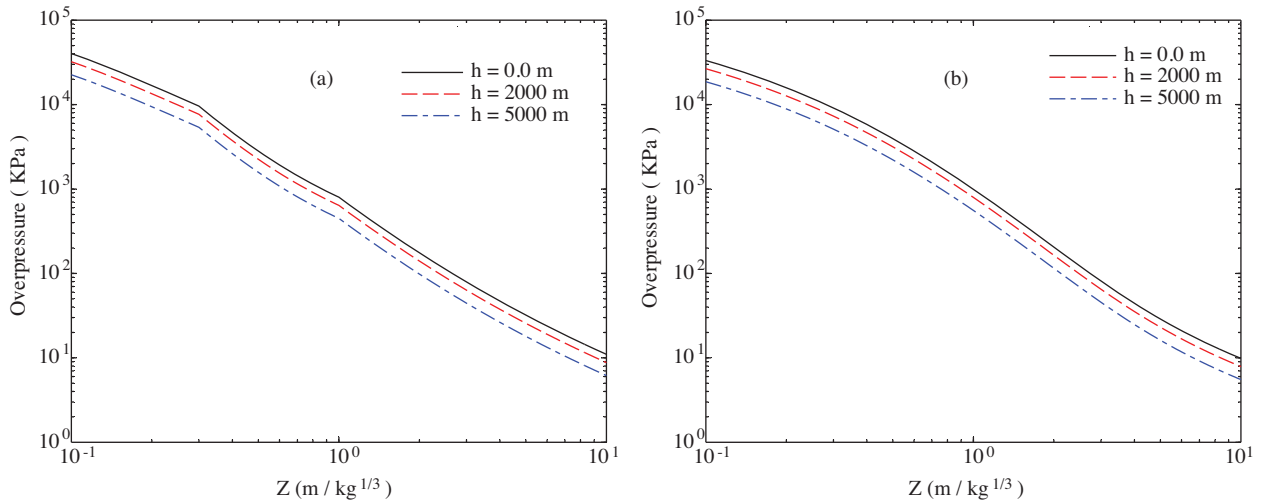
The amount of ambient pressure and air density for 7 different elevations are presented in Table 4, and the internal energy in all conditions is 0.2068 kJ/g. In order to estimate the overpressure in this condition a 1 kg spherical charge is used, considering that all of the physical and geometrical conditions are exactly the same as previous conditions, and only ambient pressure and density vary.

**Table 4.** Ambient pressure and air density at various elevations above sea level.

Elevation above sea level (m)	$P_0$ (Pa)	Density (kg/m <sup>3</sup> )
0	101,332	1.225
500	95,509	1.15461
1000	90,020	1.08826
1500	84,847	1.02572
2000	79,972	0.966782
3000	71,045	0.858865
5000	56,069	0.677825

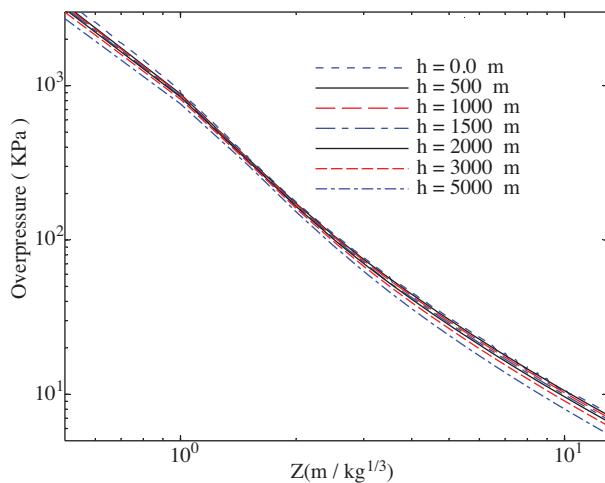
**Maximum overpressure**

Figure 17 shows the standard double logarithmic plot of maximum overpressure versus the scaled distance ( $Z$ ) under the mentioned conditions in Table 4. In this plot, all curves seem to be very close to each other, but this is partially because of the logarithmic scale used. Therefore, a difference between the results due to the difference in elevation is noticeable.



**Figure 16.** Maximum overpressure versus scaled distance for 3 different elevations: a) Henrych; b) Kinney-Graham.

In Figure 18, the pressures calculated from the simulation in altitude equal to 5000 m are compared with those from the Henrych and Kinney-Graham equations. It can be seen that the difference between the simulation and existing equations is very large. According to Figure 18, it is obvious that the results of the simulation do not prove the results of the Kinney-Graham and Henrych equations. Consequently, it is necessary to develop a mathematical relationship that is able to deal with the effects of altitude.



**Figure 17.** Maximum overpressure versus scaled distance at various heights (numerical results).

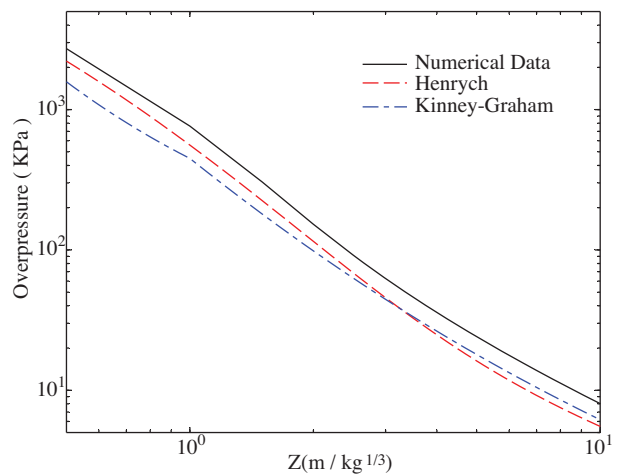


**Figure 18.** Comparison of maximum overpressure calculated from simulating with Henrych and Kinney-Graham equations in altitude equal to 5000 m.

Parameter  $\Delta$ , which is derived from the following equation, has been defined in order to calculate the effects of altitude.

$$\Delta = \frac{\left(\frac{p_s}{p_0}\right)_h - \left(\frac{p_s}{p_0}\right)_0}{\left(\frac{p_s}{p_0}\right)_0} \quad (12)$$

In this equation, subscripts  $h$  and  $0$  represent altitude and the bench mark at sea level, respectively. Therefore, to calculate the maximum overpressure at any given elevation the coefficient must be added to  $P_s/P_0$  as follow;:

$$\left(\frac{p_s}{p_0}\right)_h = \left(\frac{p_s}{p_0}\right)_0 \times (1 + \Delta) \quad (13)$$

If  $\Delta$  is considered to be zero (unmodified condition), the maximum overpressure ( $P_s$ ) calculated from Eq. (13) would be less than the actual value. The data prove that the value of  $\Delta$  depends on 2 factors;  $Z$  and  $h$ , and to make it simpler  $\Delta$  can be written as follow;:

$$\Delta = F(z) \cdot G(h) \quad (14)$$

At every elevation, by dividing resulting  $\Delta$  for different  $Z$ 's by amount of  $\Delta$  for  $Z = 0.5$  (arbitrary case),  $F(z)$  can be calculated. In Figure 19,  $F(z)$  is shown for different  $Z$ 's at different elevations. It can be seen that all of the curves can be replaced with only one suitable average approximation. For calculating  $F(z)$ , a multi curve (Eq. (15)) is fitted to an average approximation of numerical results (Figure 20).

$$\begin{aligned} F(z) &= 1.227 + 0.756 \log_{10} Z && ; \quad Z \leq 1.5 \\ F(z) &= 0.42 [\log_{10} Z]^2 - 1.22 \log_{10} Z + 1.561 && ; \quad 1.5 \leq Z \leq 20 \\ F(z) &= 0.7 && ; \quad Z \geq 20 \end{aligned} \quad (15)$$

Moreover, as it can be seen in Figures 19 and 20, the value of  $F(z)$  is at its maximum in the vicinity of  $Z = 1.5$ . Actually, in this domain the fluctuation in the elevation does not have a great effect on maximum overpressure. Therefore, in this case the bench mark overpressure data can be used for calculation with acceptable approximation.

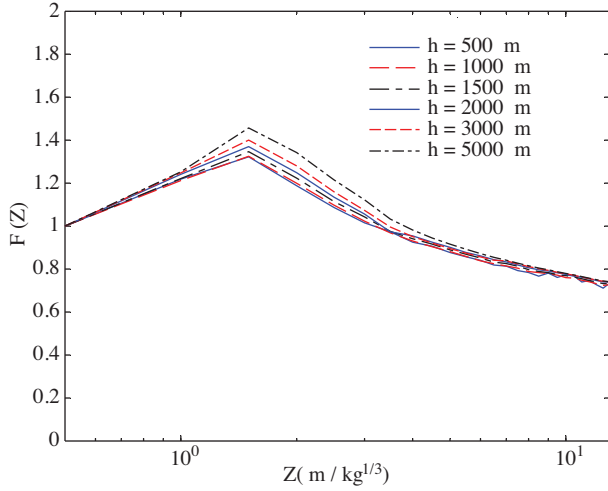
$G(h)$ , which is the value of  $\Delta$  for  $Z = 0.5$  at different elevations, is shown in Figure 21. As can be seen in this figure,  $G(h)$  can be considered as one straight line. The equation of this line is;

$$G(h) = 8.3 \times 10^{-5} h \quad (16)$$

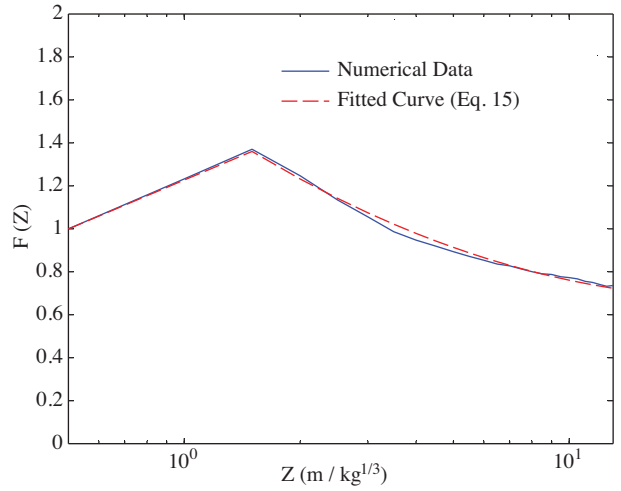
Therefore, to determine the maximum overpressure at different altitudes, it is necessary that the above coefficients be applied for any bench mark of overpressure, such as the Kinney-Graham equations or TM5-1300 graph, or suggested Eq. (8).

Figure 22 shows the importance of considering the modified parameter  $\Delta$  in the maximum overpressure estimation above sea level.

Overpressure calculated by Eq. (13) is called modified pressure if  $\Delta$  is considered non-zero and unmodified pressure if  $\Delta$  is considered zero. In Figure 22, modified pressure, unmodified pressure, and actual value of maximum overpressure numerically calculated at an altitude of 5000 m above sea level are compared. As can be seen, the usage of modified parameter  $\Delta$  for overpressure estimation is necessary.



**Figure 19.**  $F(z)$  versus scaled distance at various heights (numerical results).



**Figure 20.** Comparison of Eq. (8) and mean of  $F(z)$  at various heights.

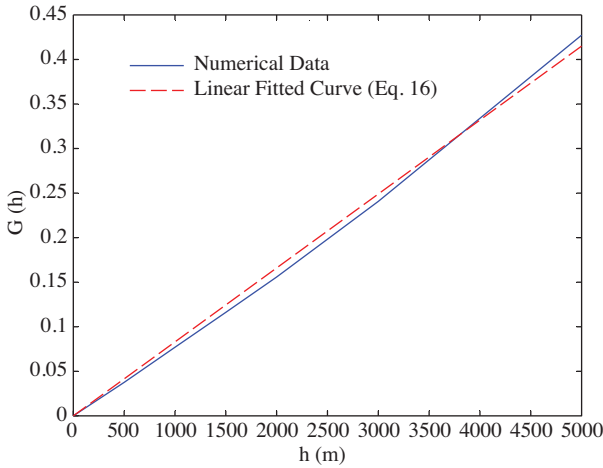


**Figure 21.** Comparison of Eq. (16) and  $G(h)$ .

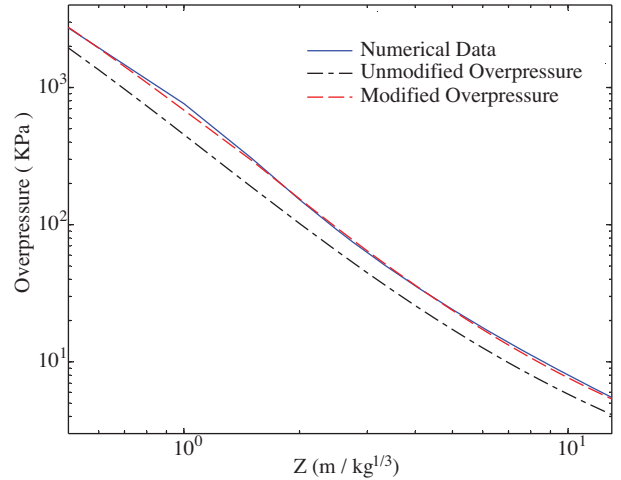


**Figure 22.** Comparison of unmodified and modified maximum overpressure and numerical data at altitude of 5000 m above sea level.

**Positive phase duration**

Duration is calculated in 6 different altitudes and is drawn in Figure 23. As can be seen in this figure, changes in altitude in different ranges of  $Z$  affect  $T_s$  differently. In a certain region, it causes  $T_s$  to decrease and in a different region causes it to increase. As seen in Figure 23, with increasing altitude, the difference of duration with standard situation is increased. In  $Z$ 's smaller than 2.5, duration shows such a different manner to the change of altitude, which makes the prediction of duration in different altitudes very difficult. In  $Z$ 's higher than 2.5, duration increases as a result of the increase in altitude; as such at an altitude of 5000 (m) its increase is limited to 10%.

Therefore, according to unordered changes and small duration in various altitudes, there is no need to develop a new relation of modification of  $T_s$  in different altitudes.

### Positive impulse

Impulse values with respect to different altitudes are drawn in Figure 24. As seen in this figure, impulse values in the  $Z < 0.2$  range, with respect to different altitudes are approximately the same. In the range of  $Z > 0.9$ , impulse curves are parallel to each other. In the range of  $0.2 < Z < 0.9$  there is a great difference between impulse values. Hence, Eq. (17) is proposed in order to consider the effect of altitude above sea level:

$$(I_m)_h = \lambda (I_m)_0 \quad (17)$$

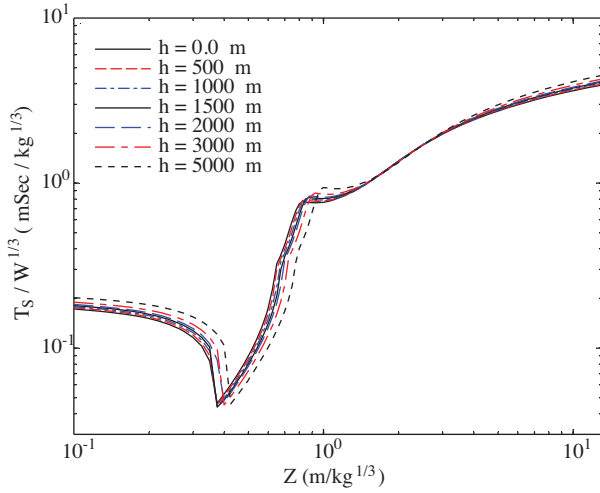


**Figure 23.** Positive phase duration for different altitudes.

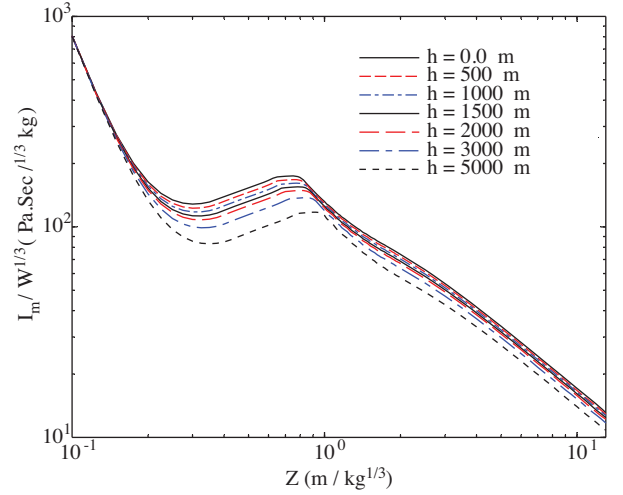


**Figure 24.** Positive impulse for different altitudes.

Coefficient  $\lambda$  is a function of height ( $h$ ) and  $Z$ , which is found by dividing the impulse values of different altitudes to the corresponding values in sea level.

It is seen in Figure 25 that in larger  $Z$ 's  $\lambda$  is approximately independent of  $Z$ , but in smaller  $Z$ 's, especially in the range of  $0.2 < Z < 0.9$ ,  $\lambda$  depends on  $Z$ , in addition to  $h$ . Therefore,  $\lambda$  can be expressed by 2 functions;  $K(h)$  and  $L(Z, h)$ .

The average values of  $\lambda$  in different  $Z$ 's are calculated and drawn in Figure 26. This curve can be linearly approximated by Eq. (18):

$$K(h) = 1 - 0.03655 h \quad (18)$$

In the above equation  $h$  is in km.

In Figure 27,  $\lambda$  values are normalized with respect to mean values. In the  $0.2 < Z < 0.9$  range, changes in  $\lambda$  are greater with respect to  $Z$  and in all other ranges this relationship is less or even negligible. Thus, Eq. (19) is proposed for calculating values of  $L(Z, h)$ :

$$\begin{aligned} L(Z, h) &= 0.4080 h Z^2 - 0.465 h Z + 0.077 h + 1; & 0.2 \leq Z \leq 0.9 \\ L(Z, h) &= 1; & Z > 0.9 \end{aligned} \quad (19)$$

According to the above explanations,  $\lambda$  can be approximated by Eq. (20):

$$\begin{aligned} \lambda &= 1; & Z < 0.2 \\ \lambda &= L(Z, h) \times K(h); & Z \geq 0.2 \end{aligned} \quad (20)$$

In Figure 28, exact values of impulse at 5 km altitude, which are calculated by numerical simulation, are compared with the values of impulse calculated by Eqs. (17) – (20). In this comparison  $I_m$  is calculated by Eq. (8). It is seen that impulse values are correctly calculated at different altitudes using the modification factor.

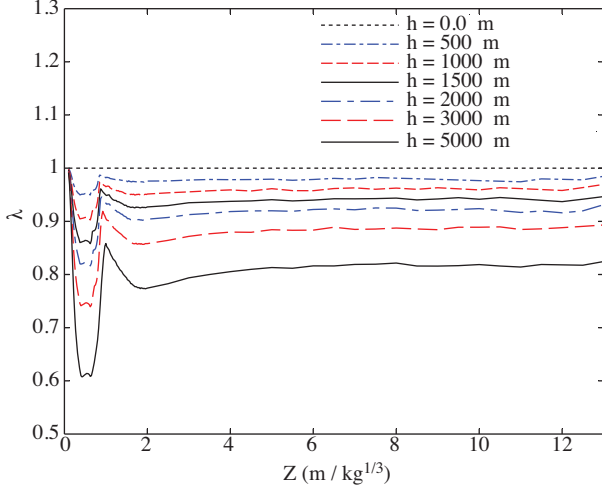


**Figure 25.**  $\lambda$  versus scaled distance at various heights (numerical results).

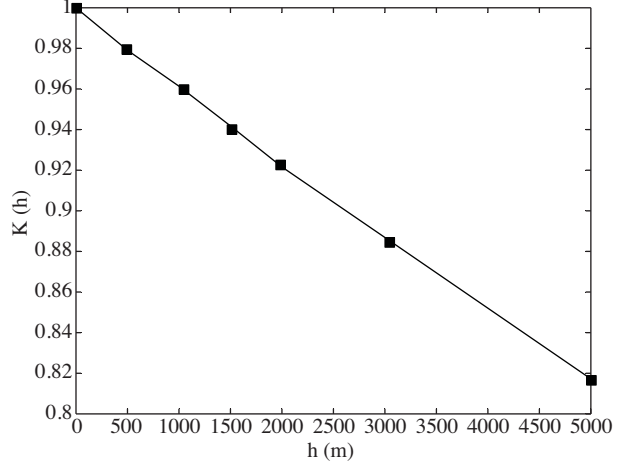


**Figure 26.**  $K(h)$  values versus altitude.

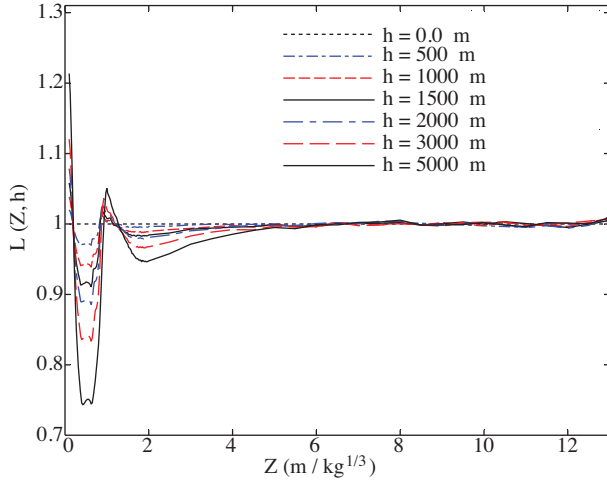


**Figure 27.**  $L(Z, h)$  value versus  $Z$  at different altitudes.

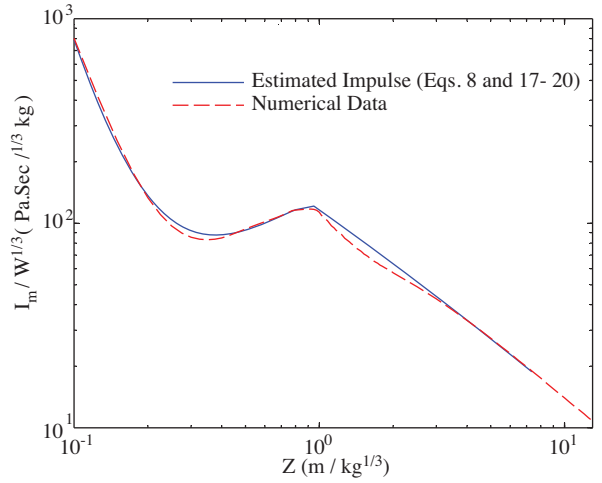


**Figure 28.** Comparison of modified impulse obtained by Eq. (8) and numerical data at altitude of 5000 m above sea level.

**Conclusion**

In this paper, the explosion phenomenon and blastwave propagation in air are numerically simulated and blast-wave parameters are calculated using AUTODYN-1D software. Maximum overpressure, positive phase duration, and positive impulse values, which are calculated by numerical simulation, are compared with experimental data and equations presented by other researchers and are verified. By fitting curves on numerical results, Eqs. (5,



(7), and (8) are proposed to calculate the maximum overpressure, positive phase duration, and impulse values, and show high accuracy.

In addition, the effect of ambient pressure on various blastwave parameters is investigated. It is shown that the overpressure at altitudes higher than sea level is less than the overpressure in sea level. This decrease can be calculated by Eq. (13), using parameter  $\Delta$ , which is calculated by Eqs. (14)–(16).  $T_S$  values derived by numerical simulations show that the effect of ambient pressure in various  $Z$ 's differs, but this difference is small and can be neglected. Numerical results show that the changes in altitude affect the impulse. This effect depends on  $Z$  and  $h$ . Impulse values in different altitudes can be calculated by Eq. (17), using a modification factor,  $\lambda$ , which is calculated by Eqs. (18)–(20). It is also shown in this paper that using  $\Delta$  and  $\lambda$  for calculating overpressure and impulse in altitudes higher than sea level is mandatory.

### References

- AUTODYN User's Manual, Reversion 6.1, Century Dynamics Inc., 2005.
- Bangash, M.Y.H., and Bangash, T., "Explosion- Resistant Buildings", Springer Pub., 2006.
- Black, G., "Computer Modeling of Blast Loading Effects on Bridges", M.S. Thesis in Lafayette College, Easton, Pennsylvania, 2006.
- Borgers, J.B.W. and Vantomme, J., "Towards a Parametric Model of a Planar Blastwave Created with Detonating Cord", 19th military aspects of blast and shock, Canada, Calgary, 2006.
- Bulson, P.S., "Explosive Loading of Engineering Structure", E & FN Spon, London, 1997.
- Chapman, T.C., Aros, T. and Smith, P.D., "Blast Wave Simulation Using AUTODYN2D: A Parametric Study", Int. J. Impact Engineering, 16, 777-787, 1995.
- Clutter, J.K. and Stahl, M., "Hydrocode Simulations of Air and Water Shocks for Facility Vulnerability Assessments", Journal of Hazardous Materials, 106, 9-24, 2004.
- Henrych, J., "The Dynamics of Explosion and Its Use", Elsevier, Amsterdam, 1979.
- Izadifard, R.A. and Maheri, M.R., "Application of DBD Method to Assess the Level of Structural Damage Due To Blast Loads.", Journal of Mechanical Science and Technology, in press, 2009.
- Kinney, G.F. and Graham, K.J., "Explosive Shocks in Air", Springer, 2nd Ed., Berlin, 1985.
- Krauthammer, T., "Modern Protective Structures", CRC Press, New York, 2008.
- Luccioni, B., Ambrosini, D. and Danesib R., "Blast Load Assessment Using Hydrocods", Engineering Structures, 28, 1736-1744, 2006.
- Mays, G.C. and Smith, P.D., "Blast Effects on Buildings", Thomas Telford Publications, UK, 1995.
- Shames, I.H., "Mechanics of Fluids", McGraw-Hill, Second Edition, US, 1982.
- Smith, P.D. and Hetherington J.G., "Blast and Ballistic Loading of Structures", Butterworth, Heinemann Ltd, UK, 1994.
- Sonntag, R.E., Borgnakke, G.L. and Vanwylen, G.J., "Fundamentals of Thermodynamics", John Wiley & Sons, Fifth Edition, New York, 1998.
- TM5, "Fundamentals of Protective Design for Conventional Weapons", Department of Army- TM5-855-1, US, 1987.
- TM5-1300, "Design of Structures to Resist the Effects of Accidental Explosions", Department of the Army, Technical Manual, US, 1990.
- UFC-3-340-02, "Structures to Resist the Effects of Accidental Explosions", Department of Defense, Unified Facilities Criteria, US, 2008.